MECHANIKA TEORETYCZNA
I STOSOWANA
Journal of Theoretical
and Applied Mechanics
2, 35, 1997

THERMODYNAMIC AND MECHANICAL NONEQUILIBRIUM IN FLASHING FLOW WITH A SHOCK WAVE IN LIQUID-VAPOUR MIXTURE

ZBIGNIEW BILICKI

ROMAN KWIDZIŃSKI

Institute of Fluid-Flow Machinery Polish Academy of Sciences, Gdańsk

e-mail: zb@imppan.imp.pg.gda.pl

The paper presents a theoretical model for two-phase liquid-vapour flow. The model is applied to description of the condensation within the shock wave region. Also, the experimental results of water-vapour flow with a stationary shock wave are presented where particular attention is paid to the measurements of flow parameters within the shock wave. The results of experiments support the assumptions accepted in proposed theoretical model.
Key words: two-phase flow, shock wave, critical velocity, collapse of a vapour bubble

1. Introduction

The two-phase flows define a very wide category of flows. The paper concerns two- phase one-component flow where the mixture of liquid and its vapour is a flowing medium. Most often this type of medium can be found in power plants, chemical installations as well as in high-pressure safety systems. That is why the engineers and designers of these systems endeavour to find an appropriate description of liquid-vapour flows. However, the reliable description of these flows requires comprehensive knowledge of accompanying phenomena and provides the researches with an incentive to undertake research projects into the nature of two-phase flows.

Two aims are pursued in this contribution. First, the paper presents a broad account of the results of experimental investigation into stationary shock waves in the water-vapour mixture. To the best of our knowledge these results

are unique in the literature. Second, a simple mathematical homogeneous model of two-phase flow within the shock wave region is presented. The model gives averaged distributions of flow parameters inside the region. The use of this model is generally justified in the case of bubble flow and may be extended to describe the flow with foam structures. In the case of bubble flow, the slip and temperature difference between the phases in the shock region is a considerable source of entropy production due to the viscosity and thermal conductivity of the liquid surrounding the bubbles. These effects, taking place in the mezoscopic scale, namely in the boundary layer around each bubble present in the flow, are reflected in the macroscopic scale and may be described by dissipative terms in the homogeneous model.

Those phenomena can be explained if the wavy properties of two-phase flow are taken into account. The wavy nature of the flow becomes particularly conspicuous in transonic or critical flows occurring very often due to the fact that the critical velocity of the two-phase media is relatively low and for bubble flow equals several dozens m/s, Bilicki (1996a). An additional feature of two-phase flows consists in relatively long relaxation times for the exchange of mass, momentum and energy between the phases. These relaxation times θ determine the rate at which two-phase systems revert to the state of thermodynamic equilibrium. If the relaxation time θ is of the same order of magnitude as the characteristic time for this phenomenon ϑ, then the nonequilibrium processes should be accounted for in the description of two-phase flow. For example, the time ϑ during which a fluid element of the two-phase medium passes through a region of strong pressure gradient due to a shock wave of length 20 cm is about 10^{-2} s. The characteristic time ϑ for the phenomenon of expansion in the vicinity of a throat in a convergent-divergent channel during two-phase flow at an around-critical velocity is of the same order. In both cases the thermodynamic nonequilibrium should be taken into consideration while describing the flow. Otherwise, the obtained profiles of parameters and their evolution are far from the reality even qualitatively. It is believed that the thermodynamic nonequilibrium is important for flow modelling if the Deborah number defined as (cf Kestin (1993))

$$\mathrm{De} = \frac{\vartheta}{\theta}$$

is $\mathrm{De} > 0.1$.

This paper deals with flows where $\mathrm{De} > 0.01$. Thermodynamic nonequilibrium in two-phase flows means that the average or local temperatures of the liquid T_l and the vapour T_g are not the same and that the average or local hydrodynamic pressure P^h in the two-phase medium differs from the

corresponding thermodynamic pressure P. Due to the difference between the temperatures of the liquid and the vapour the actual dryness fraction x differs from the equilibrium dryness fraction $\overline{x}$. The actual dryness fraction is an easily measurable quantity. In practice, it is impossible to measure the difference between the pressures P and P^h. The latter can be measured using a manometer or pressure tube and is equal to the former only in the case of incompressible media, that is when the velocity divergence disappears, which does not occur in two-phase flows. The difference between P and P^h is proportional to the divergence of the barycentric velocity of the two-phase system and the linear coefficient is called the second viscosity ζ. The second viscosity can be sometimes larger than the molecular viscosity μ, especially for dense compressible media like two-phase media, see Landau and Lifszic (1958).

Irreversible thermodynamic transitions which take place in the fluid element after withdrawing external forces bring the system back to the state of thermodynamic equilibrium. These irreversible thermodynamic transitions occurring during two-phase flows are the source of entropy production. It is an important research problem how to put them into the governing equations of two-phase flows. The problem is of particular significance in view of the fact that the two-phase medium, as a rule, is a non-continuum described by means of equations for continua. During the transformation from the non-continuous to continuous system it is necessary to preserve characteristic features of the two-phase system including the factors responsible for dissipation of energy due to irreversible thermodynamic processes. From this point of view the two-phase medium can be treated as a continuous medium with an internal structure. Let us now investigate to what degree the internal structure of two-phase flow can be represented in the description of two-phase flow by means of a continuous model. Let us demonstrate two different cases.

The first one is the flow of a liquid undergoing spontaneous evaporation. This flow is referred to as flashing flow and is described by means of a continuos relaxation model. The thermodynamic nonequilibrium due to the temperature difference between the phases is pronounced by the difference between the actual and equilibrium dryness fractions. It can be anticipated that this type of thermodynamic nonequilibrium is decisive for the properties of the two-phase one-component flow through the nozzle.

The second case is the two-phase bubble flow through the stationary shock wave where the condensation takes place. In order to describe this case two sources of energy dissipation are distinguished. The first source is due to the shear stress and the second one due to the heat conduction along the flow.

2. Modelling of two-phase flow by means of a continuous relaxation model

In order to describe multi-phase flows, including two-phase flows, the methods of continuum mechanics, see Truesdell and Noll (1965), are widely applied and transferred onto the grounds of multi-phase flows by incorporating the concept of a multi-velocity continuous medium and mutual penetration of different phases. In the case of two-phase media this resolves itself into the assumption that a given point in space can belong to both phases, each phase having its own velocity and different physical parameters including density, specific enthalpy and temperature. In keeping with the properties of continuum the parameters of each phase make up continuous fields. This method is used by the so-called two-fluid model widely used for modelling two-phase media. A disadvantage of this model is the fact that it requires 56 closure equations in a one-dimensional approach and 48 in a two-dimensional approach, see Drew and Wood (1986). Therefore, it is worth looking upon the two-phase medium from a different point of view as a continuum with an internal structure. This concept seems to be a valuable alternative for the two-fluid model. Besides, the same transformation procedure from the non-continuous to continuous medium can be applied bearing in mind that an infinitesimal fluid element comprises both phases and its properties reflect its structure, Bilicki (1983). This way the physical properties of the two-phase medium; like, the relaxation time θ, thermal conductivity, viscosity will carry weight of operative quantities depending on the structure of two-phase flow, or generally on the internal structure described on the mezoscopic level, Bilicki (1996b).

The simplest model treating the two-phase medium as a medium with the internal structure is the nonequilibrium relaxation model (HRM) put forward by Bilicki et al. (1990). The model incorporates the thermodynamic nonequilibrium in the form of difference in the local temperature between the phases T_l and T_g at the infinitesimal level of a two-phase fluid element. Due to the temperature difference, the local dryness fraction x defined at the same infinitesimal level has a different value than the corresponding equilibrium dryness fraction $\overline{x}$. The above model with respect to one-dimensional flow through a channel is described by the following equations:

— The mass conservation equation

$$\frac{D\rho}{Dt} + \rho\frac{\partial w}{\partial z} = -\frac{\rho w}{A}\frac{\partial A}{\partial z} \tag{2.1}$$

— The momentum conservation equation

$$\rho \frac{Dw}{Dt} + \rho \frac{\partial P}{\partial z} = -\frac{C\tau}{A} \tag{2.2}$$

— The energy conservation equation

$$\frac{Dh}{Dt} - \frac{1}{\rho}\frac{DP}{Dt} = \frac{C\tau w}{\rho A} \tag{2.3}$$

— The evolution equation for the dryness fraction

$$\frac{Dx}{Dt} = -\frac{x - \bar{x}}{\theta_x} \tag{2.4}$$

where

$$\frac{D}{Dt} = \frac{\partial}{\partial t} + w\frac{\partial}{\partial z} \tag{2.5}$$

The evolution equation (2.4) originates from the theory of internal parameters which enables one to obtain the relationships for the internal parameters describing thermodynamic nonequilibrium of the medium, Bilicki (1994). In the case of HRM, the actual dryness fraction x assumes the role of an internal parameter. According to this theory, an internal parameter α_i is linked to other thermodynamic parameters α_i of state, including the temperature of medium T, and their gradients and high-order derivatives, generally by means of a first-order differential equation with respect to time

$$\dot{\alpha}_i = f(T, \alpha_i, a_i, \nabla T, \nabla a_i, \ldots) \tag{2.6}$$

The following quantities appear in the above equations: the barycentric velocity w expressed by the formula

$$w = \frac{w_l(1 - \varphi)\rho_l + w_g \varphi \rho_g}{\rho} \tag{2.7}$$

where the subscript l stands for the liquid, g for the vapour and φ is the void fraction (the volume ratio of the vapour phase in the fluid). The void fraction is related to the dryness fraction by the formula

$$\varphi = \frac{x\rho}{\rho_g} \tag{2.8}$$

where the density of two-phase medium ρ is

$$\rho = \rho_l(1 - \varphi) + \rho_g \varphi \tag{2.9}$$

The other quantities in Eq (2.6) are the thermodynamic pressure P, enthalpy h, cross-section of the channel A, wall shear stress τ

$$\tau = \frac{1}{2} f w^2 \rho \tag{2.10}$$

where f is an empirical friction coefficient.

The state equation accounting for thermodynamic nonequilibrium in the present model is of the form

$$h = h(\rho, P, x) = x h''(P) + (1 - x) h_L[P, T_L(P, \rho, x)] \tag{2.11}$$

where h'' is the enthalpy at the saturation line $x = 1$, in keeping with the assumption that the vapour phase is under the saturation conditions. The other quantities, like ρ'' are also assumed to correspond to the saturation line $x = 1$. The above set of equations has to be supplemented with an expression for the relaxation time θ_x. Such expressions in the form of correlations were worked out by Downar-Zapolski (1993) and Downar-Zapolski et al. (1996). Besides, also based on experimental data, the superheat of the liquid necessary for the onset of flashing was established. It was found that this superheat in the Moby Dick experiments carried out by Reocreux (1974) was between 2.5 and 3.0 K.

It should be underlined that the results of calculations by means of HRM agree well with the Moby Dick experiments, see Bilicki et al. (1990). A comparison of theoretical and experimental results is presented in Fig.1.

The physical properties of HRM were discussed in detail by Bilicki and Kestin (1990), with an analysis of entropy production in the two-phase medium described by HRM. It was established that the entropy production due to the thermodynamic nonequilibrium is

$$T \frac{Ds}{Dt}\Big|_{x \neq \bar{x}} = -(\mu_g - \mu_l) \frac{Dx}{Dt} \equiv \frac{l(\mu_g - \mu_l)^2}{\rho} \equiv \frac{\rho}{l} \left(\frac{Dx}{Dt}\right)^2 \equiv \frac{\rho}{l} \left(\frac{x - \bar{x}}{\theta_x}\right)^2 \tag{2.12}$$

where

l – phenomenological coefficient

μ_g, μ_l – chemical potentials of the vapour and the liquid, respectively.

During expansion the chemical potential of the superheated liquid is always higher than that of the vapour, which gives rise to the production of the vapour phase in the two-phase medium, that is $Dx/Dt > 0$. The entropy production due to the thermodynamic nonequilibrium ($x \neq \bar{x}$) depends on the relaxation

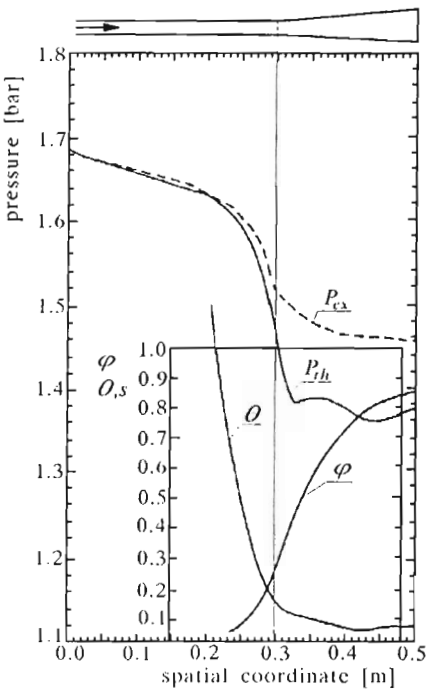

Fig. 1. The comparison of numerical investigations and Moby Dick experiments (run 402); $G = \rho w = 6496\,\mathrm{kg/m^2s}$, $T = 116.7°\mathrm{C}$; P_{ex} – measured pressure distribution, P_{th} – HRM-calculated pressure distribution, θ – calculated relaxation time θ_x, φ – measured void fraction (Bilicki et al. (1990))

time θ_x and the level of thermodynamic nonequilibrium. The total entropy production in the two-phase medium described by HRM equals

$$T\frac{Ds}{Dt} = \frac{\tau C w}{A\rho} + \frac{\rho}{l}\left(\frac{x-\overline{x}}{\theta_x}\right)^2 \tag{2.13}$$

The first term on the right-hand side of Eq (2.13) is due to the friction against the walls and is usually negligibly small compared to the entropy production due to the thermodynamic nonequilibrium.

In order to find the relationship between the relaxation time and the internal structure of the medium, Bilicki et al. (1996a) made an effort to evaluate θ_x in a theoretical way.

Now let us concentrate on the second case that is the stationary shock wave.

3. Experimental setup

In the experiment, the stationary shock wave is observed during the supercritical water-vapour flow in a vertical straight tube past an expansion nozzle. The flow velocity decreases with the distance and takes subcritical values in a narrow region, where a significant pressure rise and intense condensation are observed. Concluding, in this region a shock wave of finite width and complex internal structure appears. This shock wave is called stationary because its strength and width do not vary in time provided that flow conditions before the expansion nozzle are kept constant. The location of the shock wave, i.e. the distance from the nozzle, is also fixed under such conditions.

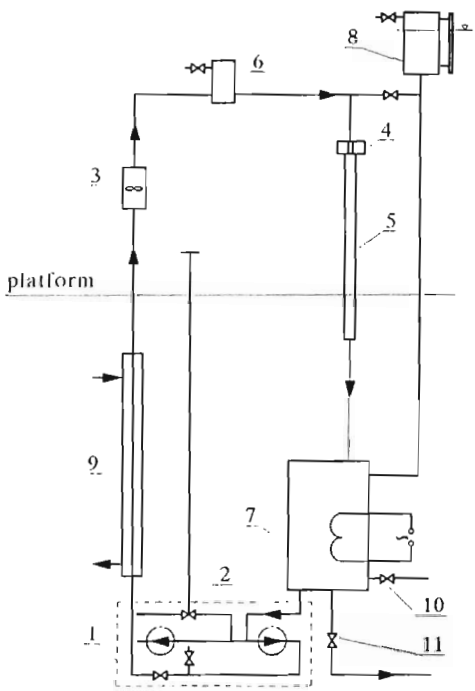

Fig. 2. Scheme of the experimental stand: 1 – pump system, 2 – flow rate control valve, 3 – flow meter, 4 – expansion nozzle, 5 – test section, 6 – air escape, 7 – heater, 8 – excess water tank, 9 – cooler, 10 – drainage valve, 11 – filling valve

A schematic diagram of the experimental setup is shown in Fig.2. Essentially, the stand consists of a closed-circuit pipeline filled with water. The circulation of water in the circuit is induced by a system of two pumps (1) connected in a series to obtain the required flow rate. The flow rate is con-

trolled by a valve (2) and the actual volumetric flux is measured by a rotary meter (3). An expansion nozzle (4) is located at the beginning of a vertical downward flow. The diameter of the throat, equal to 14.3 mm, was chosen in a way to cause a pressure drop and spontaneous boiling of the liquid. Simultaneously, the velocity of the flow increases. The resulting supercritical two-phase flow may be observed in a perspex tube (5) of internal diameter 32 mm. A heater (7) and air escape (6) are used to remove dissolved gas from the water. An excess water tank (8) assures complete fill of the loop. The constant temperature of the circulating water is maintained with the help of a cooler (9). Valves (10) and (11) are used for filling and emptying the pipeline, respectively.

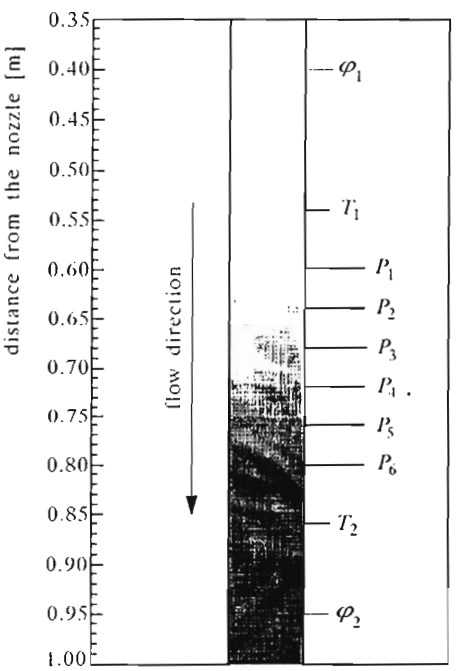

Fig. 3. Arrangement of the measurement points: P – pressure, T – temperature, φ – void fraction

The shock wave, which forms in the test section (5) for a sufficiently high flow rate, separates the two-phase flow from the flow of the liquid. Six pressure sensors are installed in the region where the shock wave is located. The arrangement of measurement points is given in Fig.3. At each point the pressure can be measured by a U-tube mercury manometer or by piezoelectric sensors PCB HM 105. The U-tube manometers are used to measure the average static

pressure. Fluctuations of the mercury level up to 60 mmHg were observed at some points located inside the shock wave. The piezoelectric sensors are used to record instantaneous fluctuations of pressure relative to the average value. The output from the sensors is recorded by means of an analogue-digital acquisition system at the maximum sampling frequency of 500 kHz. The maximum length of a record is 65536 samples with resolution of 12 bits.

Besides the pressure, additional measurements of the temperature and void fraction can also be taken at two points, located at low and high pressure sides of the shock wave (see Fig.3), respectively. The used thermocouples allow the determination of temperature with the accuracy of 0.5°C. The average void fraction is measured with the use of a capacity sensor, Jaworek (1991). This technique enables the estimation of the average void fraction in the channel section of approximate length 100 mm with accuracy of 10%.

4. Experimental results

The location and strength of shock wave depends on the actual flow rate, the temperature of the circulating water and – to a degree – on the atmospheric pressure. For the present configuration, the distance between the expansion nozzle and the shock region, and thus the length of a stretch where the two-phase flow is observed, is about 0.8 m at maximum. During the measurement series the flow parameters before the expansion nozzle are kept constant, so the location, strength and width of the shock wave are also constant. The shock wave is placed in the section covered with the sensors when the flow rate G ranges from 0.278 to 0.287 m^3/min. The shock strength does not change significantly in this range of flow rate; the pressure rise is then equal to 1.5 bar and the shock width is about 0.2 m.

The profile of average pressure, obtained for $G = 0.2835\,m^3/min$ and the average temperature of water $T_L = 20°C$, is shown in Fig.4. The void fraction in the two-phase flow before the shock region, at the distance of 0.4 m from the nozzle, was about 0.8. Inside the shock wave intense condensation of the vapour takes place. The void fraction in this region drops below 0.1. A dozen of centimetres past the shock wave it equals almost zero and few bubbles are visible there. The temperature difference on both sides of the shock region is below the measurement accuracy, i.e. is less than 0.5°C.

When the measurements of average pressure were completed, the U-tube manometers were replaced with piezoelectric sensors and pressure pulses were recorded. The pulse amplitude and frequency of occurance depend on the

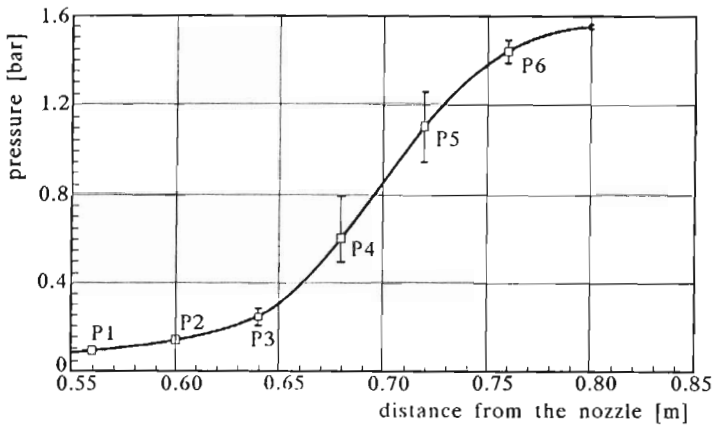

Fig. 4. The profile of average pressure measured in the stationary shock wave; $G = 0.2835\,\mathrm{m}^3/\mathrm{min}$, $T_L = 20°\mathrm{C}$. The intervals indicated on the curve show the level of pressure fluctuations measured by U-tube manometers. The points P1 ÷ P6 denote the average pressure during the measurements of pressure pulses, shown in Fig.5 and Fig.6

location in the shock wave. The points where the pulses were observed are plotted in Fig.4 against the average pressure. Typical records of pressure fluctuations at these points are presented in Fig.5 ÷ Fig.8. Similar records were obtained in experiments on noise generated by travelling cavitation (Kumar and Brennen (1993)). Therefore, it is considered that the pressure pulses are produced due to the collapse of vapour bubbles passing through the shock wave region. During the final stage of the collapse a spherical shock wave is generated that propagates through the two-phase medium and can be detected as a sharp high pressure pulse when it reaches the sensor. It follows from Fig.5 and Fig.6 that most of the bubbles collapse inside the shock region when the average pressure in their vicinity reaches a value of about $0.5 \div 1.0\,\mathrm{bar}$. The amplitude of some pulses in this region may exceed 70 bars. The time interval between the pulses is of the order of $10 \div 100\,\mathrm{ms}$. The pressure pulses are also present at the low and high pressure edges of the shock wave but they are generally of smaller amplitude and do not occur so frequently.

A more detailed view on the shape of the pulse is given in Fig.7 and in Fig.8. As in the case of bubble cavitation, two features of the pressure pulses are recognised: rebounding and multipeaking. The rebounding refers to an observation that the main (high) pulse is usually followed by a smaller one. This is due to the fact that the collapsing bubble does not disappear immediately but reappears for a short time as a growing bubble that soon

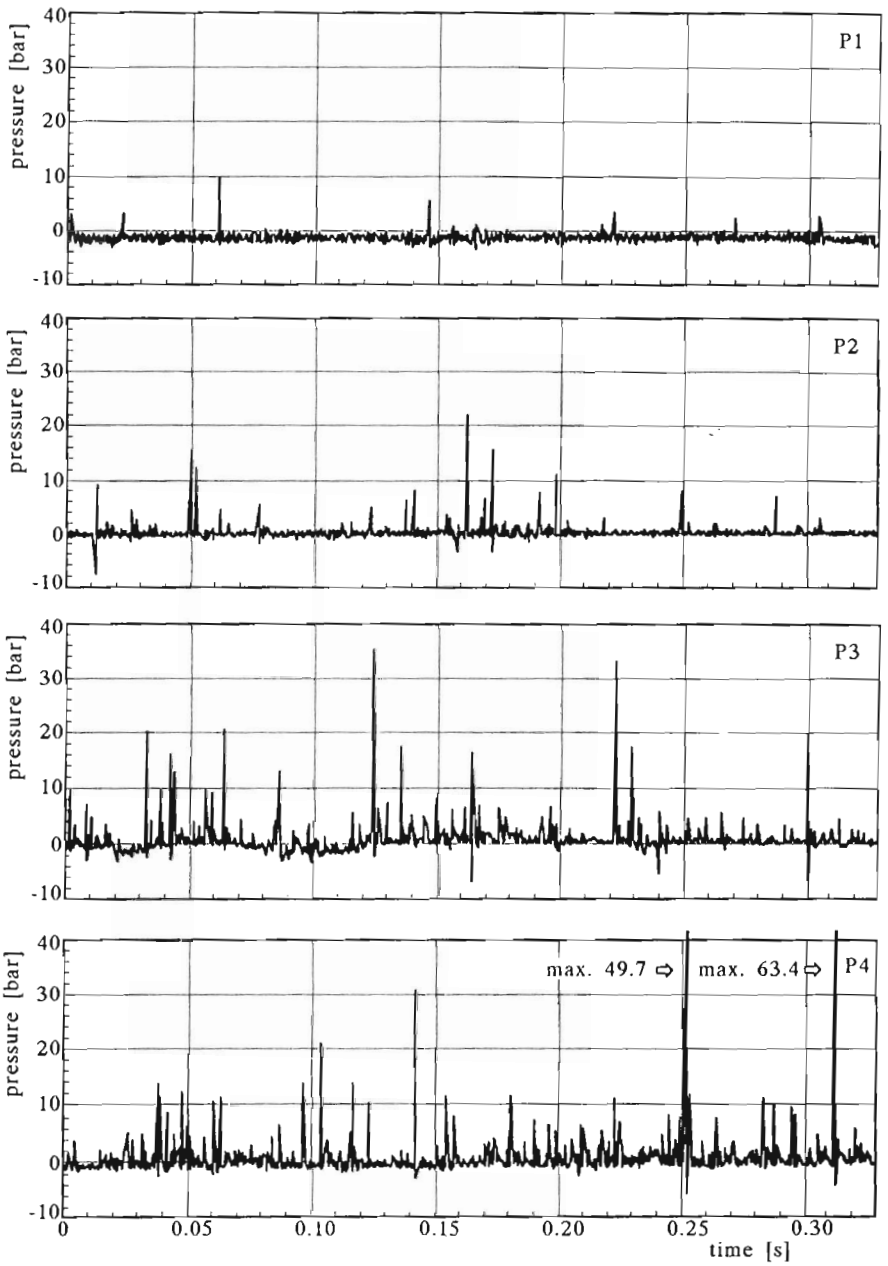

Fig. 5. Pressure pulses recorded inside the stationary shock wave. The location of measurement points is shown in Fig.4 (points P1 ÷ P4)

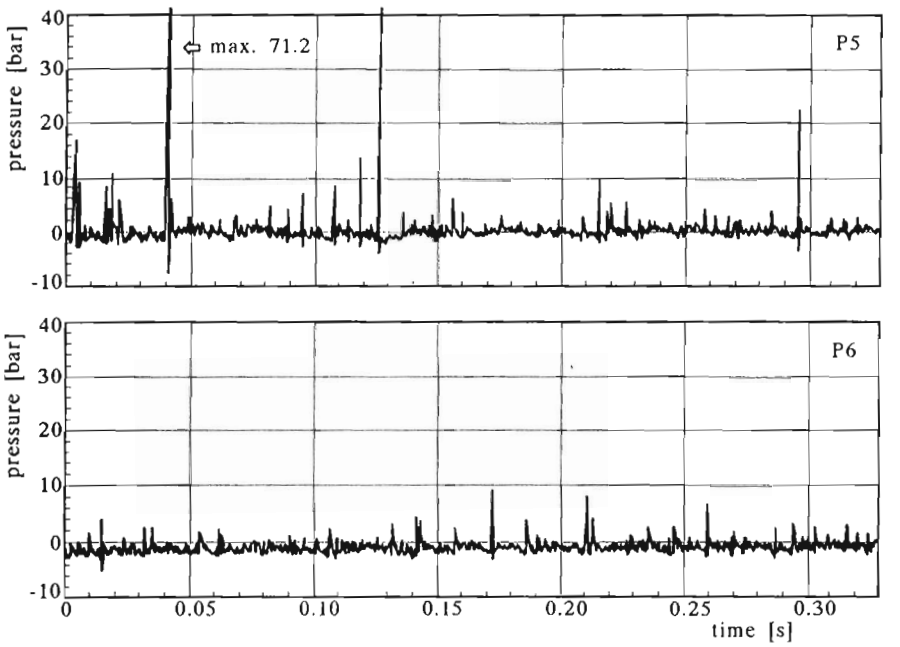

Fig. 6. Pressure pulses recorded inside the stationary shock wave. The location of measurement points is shown in Fig.4 (points P5 and P6)

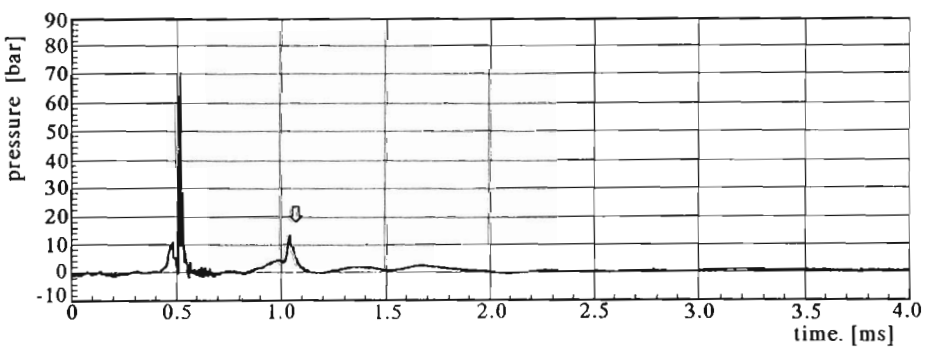

Fig. 7. An example of rebounding. The main pressure pulse (recorded at 0.5 ms) is followed by a weaker secondary pulse. The time interval between the pulses is about 0.6 ms

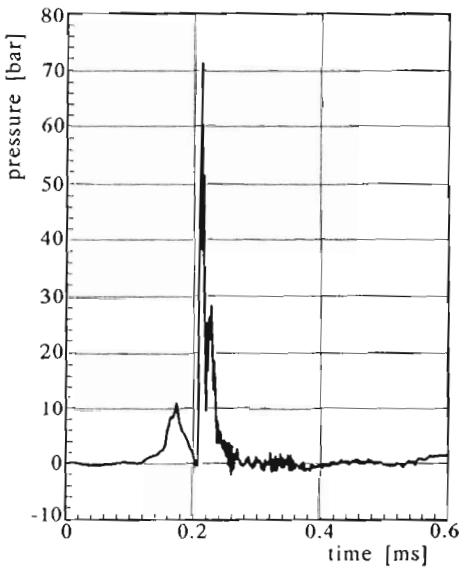

Fig. 8. An example of multipeaking. Two peaks of amplitude about 70 bars and 30 bars, respectively, can be distinguished in the main pressure pulse

starts to collapse giving rise to generation of a weaker secondary pulse (see Fig.7). The duration of the main pulse is about $0.04 \div 0.06$ ms. The time between the maximum peak in the main pulse and the maximum peak in the rebound pulse ranges from 0.5 ms to 2.8 ms. The multipeaking can be recognised in Fig.8, where it is seen that the main pulse consists of two peaks. According to Kumar and Brennen (1993), multipeaking can be the result of several mechanisms: (i) – the collapsing bubble generates microjets that are the source of multiple pressure waves; (ii) – the bubble breaks up into several pieces while collapsing; (iii) – the volume oscillations of the bubble during its collapse give rise to multiple peaks. These explanations are based on high-speed photography of the collapsing bubbles taken by several researchers.

5. Simple mathematical model

The parameters of the flow across the shock wave, averaged over a time interval greater than the duration of the pressure pulse, are constant. Thus the shock wave may be regarded as a steady phenomenon. Let us assume that the two-phase medium is considered to be a homogeneous mixture and

that the flow is one-dimensional. With those simplifications the structure of the shock wave may be described by the theory originally derived to analyse a normal shock wave in viscous and thermally conductive gases (cf Whitham (1974)). When the mass force is neglected, the fundamental equations of mass, momentum and energy balance in the general case of one-dimensional flow are in the form

$$\begin{aligned}
&\frac{\partial \rho}{\partial t} + \frac{\partial}{\partial x}(\rho u) = 0 \\
&\frac{\partial}{\partial t}(\rho u) + \frac{\partial}{\partial x}\left(\rho u^2 + P - \frac{4}{3}\mu \frac{\partial u}{\partial x}\right) = 0 \\
&\frac{\partial}{\partial t}\left(\frac{1}{2}\rho u^2 + \rho e\right) + \frac{\partial}{\partial x}\left[\left(\frac{1}{2}u^2 + e\right)\rho u + Pu - \frac{4}{3}\mu u \frac{\partial u}{\partial x} - \lambda \frac{\partial T}{\partial x}\right] = 0
\end{aligned} \tag{5.1}$$

where

ρ – density
u – velocity
P – pressure
e – specific internal energy
T – temperature
μ, λ – coefficients of dynamic viscosity and thermal conductivity, respectively.

These equations take a stationary form in the frame moving at the velocity U of the shock wave. In this new frame the spatial coordinate is calculated from

$$z = x - Ut \tag{5.2}$$

Hence

$$\frac{\partial}{\partial t} = -U\frac{d}{dz} \qquad \frac{\partial}{\partial x} = \frac{d}{dz} \tag{5.3}$$

and the balance equations can be easily integrated

$$\begin{aligned}
&-U\rho + \rho u = A \\
&-U(\rho u) + \left(\rho u^2 + P - \frac{4}{3}\mu \frac{\partial u}{\partial z}\right) = B \\
&-U\left(\frac{1}{2}\rho u^2 + \rho e\right) + \left[\left(\frac{1}{2}u^2 + e\right)\rho u + Pu - \frac{4}{3}\mu u \frac{\partial u}{\partial z} - \lambda \frac{\partial T}{\partial z}\right] = C
\end{aligned} \tag{5.4}$$

where A, B, C are integration constants. Defining the relative velocity $w = U - u$, the above set of equations can be simplified

$$\rho w = M$$

$$\rho w^2 + P + \frac{4}{3}\mu\frac{dw}{dz} = L \tag{5.5}$$

$$\left(h + \frac{1}{2}w^2\right)\rho w + \frac{4}{3}\mu w\frac{dw}{dz} + \lambda\frac{dT}{dz} = K$$

The symbols M, L, K denote integration constants, which are different from A, B, C. The enthalpy h is introduced in the energy equation. In this notation, the direction of the velocity vector $\boldsymbol{w}$ is opposite to the direction of the coordinate z. It should be emphasised that Eqs (5.5) are valid in the coordinates moving together with the shock wave. In our case, the shock wave is stationary, so $U = 0$.

It was proved by Gilbarg (1951) that there existed a unique solution of the above system of equations describing a continuous transition from a uniform state 1 at $x = -\infty$ to a different state 2 at $x = +\infty$. With nonzero coefficients of viscosity μ and heat conductivity λ, the transition takes place in the region width of which depends on actual values of the mentioned coefficients. This region is sometimes called a shock layer to distinguish it from the discontinuous solution obtained for the shock wave in non-viscous and non-conducting flow.

Far away from the shock wave the flow is uniform and the derivatives d/dz vanish. Hence, the shock relations are obtained

$$\rho_1 w_1 = \rho_2 w_2$$

$$\rho_1 w_1^2 + P_1 = \rho_2 w_2^2 + P_2 \tag{5.6}$$

$$h_1 + \frac{w_1^2}{2} = h_2 + \frac{w_2^2}{2}$$

where 1 and 2 denote the state at $z = -\infty$ and $z = +\infty$, respectively.

If we intend to adopt these equations for the flow of a two-phase homogeneous mixture we should allow for thermal nonequilibrium. It follows from experimental measurements that the temperature of water T_L does not change considerably, while it may be expected that the temperature of vapour T_V equals the saturation temperature

$$T_V = T_S(P) \tag{5.7}$$

We assume that the heat flux in the energy equation is proportional to the gradient of the vapour temperature only.

It was pointed out by Bilicki et al. (1996b) and by Kardaś (1994) that the dissipation of mechanical energy in bubble flow was mainly due to entropy production in the boundary layer around the vapour bubbles. The energy dissipation due to the slip, which is significant inside the shock region, can be taken into account by a corresponding increase in viscosity of the homogeneous two-phase mixture. Therefore, the coefficient of operative viscosity $\tilde{\mu}$ can be introduced, whose order of magnitude is estimated to be $10^5 \div 10^6$ times higher than that of the coefficient of dynamic viscosity for water (Bilicki et al. (1996b)). Due to the presence of a temperature difference between the phases inside the shock wave, a thermal boundary layer where additional dissipation takes place develops around the vapour bubbles. This phenomenon is accounted for in the homogeneous model by means of the operative heat conductivity $\tilde{\lambda}$. Its value is estimated to be $10^3 \div 10^4$ times higher than the coefficient λ for water (Kardaś (1994)). Thus the system of Eqs (5.5) for the homogeneous mixture takes the form

$$\begin{aligned} &\rho w = M \\ &\rho w^2 + P + \frac{4}{3}\tilde{\mu}\frac{dw}{dz} = L \\ &\left(h + \frac{1}{2}w^2\right)\rho w + \frac{4}{3}\tilde{\mu}w\frac{dw}{dz} + \tilde{\lambda}\frac{dT_V}{dz} = K \end{aligned} \tag{5.8}$$

The symbol w now denotes the barycentric velocity and P is the pressure, common for both phases. The density of mixture ρ is calculated from

$$\rho = \varphi\rho_V + (1-\varphi)\rho_L \tag{5.9}$$

where φ denotes the void fraction. The conservation equations (5.8) are augmented with the state equation

$$h = h(P, \rho, T_L) \tag{5.10}$$

Eqs (5.8) are valid for the flow which is uniform and in equilibrium at an infinite distance from the shock wave. The flow observed experimentally fulfils these conditions at some distance from the shock region, so we expect that the flow conditions on both sides of the shock wave should satisfy the relations (5.6). The exemplary calculations were done to confirm the experimental pressure profile shown in Fig.4. The comparison of measured flow conditions at the low-pressure and high-pressure sides of the shock wave with the values calculated from Eqs (5.6) is shown in the table below.

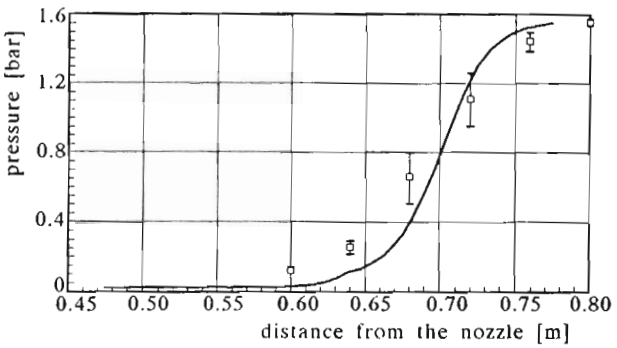

Fig. 9. Comparison of the calculated (—) and measured (□) distributions of pressure in the shock wave

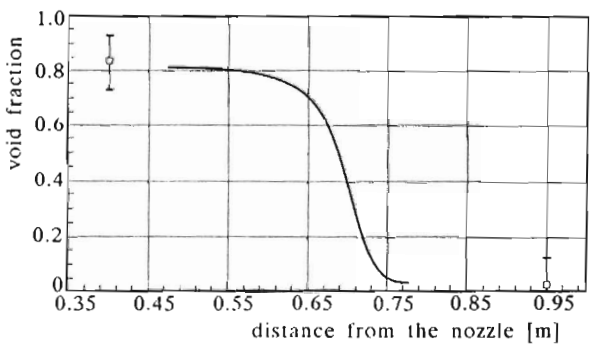

Fig. 10. Comparison of the calculated (—) and measured (□) distributions of void fraction in the shock wave

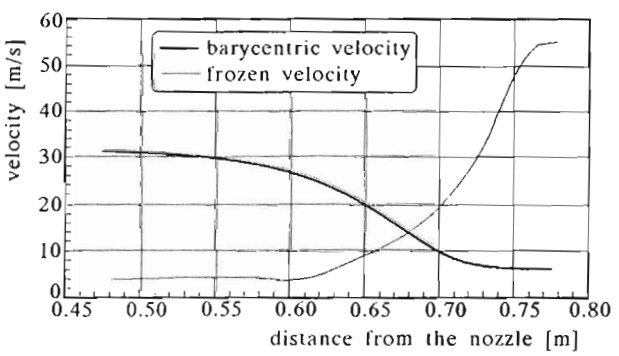

Fig. 11. The calculated velocity profile in the shock wave

Parameter	At the low-pressure side			At the high-pressure side		
	z [m]	Measured	Calculated	z [m]	Measured	Calculated
pressure [bar]	0.6	0.12135 ±0.011	0.0302	0.8	1.54505 ±0.01	1.5421
void fraction	0.4	0.829 ± 0.1	0.8116	0.95	≈ 0.015	0.0266
flow rate [m³/min]	–	0.2835 ±0.0005	0.2835		0.2835 ±0.0005	0.2835
velocity [m/s]	0.475	–	31.2321	0.775	–	6.0395
liquid temperature [°C]	0.54	20 ± 0.5	20	0.86	20 ± 0.5	20.29
vapour temperature [°C]	0.475	–	20	0.775	–	112.21

The calculated boundary conditions agree with measurements assuming that the temperature of water T_L across the shock region rises by 0.29 K. This value is smaller than our measurement accuracy, so it was not detected, but it is expected according to the Second Law of Thermodynamics. In order to solve Eqs (5.8) it was therefore assumed that the distribution of temperature T_L may be approximated by a proper sine function. The calculated distributions of pressure, void fraction and velocity are shown in Fig.9 ÷ Fig.11. These results were obtained for the operative coefficients $\tilde{\mu} = 248.35\,\mathrm{kg/m{\cdot}s}$ and $\tilde{\lambda} = 5373\,\mathrm{W/m{\cdot}K}$, i.e. $2.5 \cdot 10^5$ and $9 \cdot 10^3$ times larger then the coefficients of viscosity and heat conductivity for water, respectively. These multiplied values are in agreement with the need for increased dissipation of the homogeneous medium, which is, as already mentioned, due to the mechanical and thermal nonequilibrium existing inside the shock wave.

6. Conclusions

The stationary shock wave was observed in the supercritical flow of a water-vapour mixture. The location, strength and width of the shock wave remained constant under fixed flow conditions. The width of the shock wave was about 0.2 m and the pressure increase was 1.5 bar in this region. Inside the shock region sharp pressure pulses were detected. Their amplitude and frequency depend on the location in the shock region. The observed maximum amplitude was as high as 70 bars and the duration of an individual pulse was

about 0.05 ms. It is considered that the pressure pulses were generated by the collapsing vapour bubbles.

The pressure pulses are short-time phenomena and the parameters of the flow across the shock wave, averaged over a time interval greater than the duration of the pulse, are constant. Thus, if the two-phase medium is considered to be a homogeneous mixture, the shock wave can be regarded as a steady phenomenon. With this simplification the structure of the shock wave can be described within the framework of theory originally derived to analyse the structure of a normal shock wave in viscous and thermally conductive gases. However, the shock width calculated in this manner agrees well with experimental observations if the coefficients of viscosity and thermal conductivity are assumed to be several orders of magnitude greater than those of water or vapour. Values of the coefficients of viscosity and conductivity should be assumed large enough so as to properly represent the energy dissipation in the two-phase mixture which is due to the velocity and temperature gradients in the boundary layer around the vapour bubbles.

Acknowledgements

The financial support received from the EEC under grant ERB EV5VCT930289 is gratefully acknowledged.

References

1. BILICKI Z., 1983, Description of Two-Phase Flow Systems by Means of the Continuous Model (in Polish), *Zeszyty Naukowe IMP PAN,* 167/1066/83
2. BILICKI Z., 1994, The Concept of the Hidden Variables Theory on the Background of Contemporary Trends in Thermodynamics of Irreversible Processes Applied to Two-Phase Flow (in Polish), *Zeszyty Naukowe IMP PAN,* 421/1379/94
3. BILICKI Z., 1996a, Transonic Two-Phase Flow in Channels (in Polish), Lecture Notes, IX Summer School of Fluid Mechanics, 129-160
4. BILICKI Z., 1996b, Thermodynamic Nonequilibrium in the Two-Phase System – a Continuum with an Internal Structure, *Arch. of Thermodynamics,* **17**, 1-2, 109-134
5. BILICKI Z., KESTIN J., PRATT M.M., 1990, A Reinterpretation of the Results of the Moby Dick Experiments in Terms of the Nonequilibrium Model, *Journal of Fluids Engineering,* **112**, 212-217
6. BILICKI Z., KESTIN J., 1990, Physical Aspects of the Relaxation Model in Two-Phase Flow, *Proc. Royal Society London* A, **428**, 379-397
7. BILICKI Z., KWIDZIŃSKI R., 1995, Literature Survey on the Shock Wave Structure in Two-Phase Flow, EEC Report No. 1, Institute of Fluid Flow Machinery, Gdańsk

8. BILICKI Z., KWIDZIŃSKI R., MOHAMMADEIN S.A., 1996a, Evaluation of the Relaxation Time of Heat and Mass Exchange in the Liquid-Vapour Bubble Flow, *Int. J. Heat Mass Transfer*, **39**, 753-759

9. BILICKI Z., KWIDZIŃSKI R., MICHAELIDES E.E., 1996b, Effect of Mechanical Non-Equilibrium on Dissipation in Condensing Bubble Flow, *Arch. of Thermodynamics*, **17**, 1-2, 25-33

10. DOWNAR-ZAPOLSKI P., 1993, An Influence of the Thermodynamic Disequilibrium on the Pseudo-Critical Flow of One-Component Two-Phase Mixture (in Polish), Ph.D. Thesis, Institute of Fluid Flow Machinery, Polish Academy of Sciences, Gdańsk, Poland

11. DOWNAR-ZAPOLSKI P., BILICKI Z., BOLLE L., FRANCO J., 1996, The Non-Equilibrium Relaxation Model for One-Dimensional Flashing Liquid Flow, *Int. J. Multiphase Flow*, **22**, 473-483

12. DREW D.A., WOOD R.T., 1986, Overview and Taxonomy of Models and Methods, *Proc. of The First International Workshop on Two-Phase Flow Fundamentals*, September 22-27, 1985 Gaithersburg, MD, USA

13. GILBARG D., 1951, The Existence and Limit Behavior of the One-Dimensional Shock Layer, *Am. J. of Math.*, **73**, 256-274

14. JAWOREK A., 1991, Void Fraction Measurements in Two-Phase Flow by Means of Capacity Transducer (in Polish), Institute of Fluid Flow Machinery, Report No. 180/91

15. KARDAŚ D., 1994, Analysis of Influence of the Dissipative Terms on Numerical Solution of Nonsteady Two-Phase Flow (in Polish), Ph.D. Thesis, Institute of Fluid Flow Machinery, Gdańsk

16. KESTIN J., 1993, Thermodynamics (An essay), In *Problems of Fluid-Flow Machines*, Edit. Z.Bilicki et al., Issue of the Institute of Fluid-Flow Machinery, Polish Academy of Sciences, Gdańsk, 319-334

17. KUMAR S., BRENNEN C. E., 1993, A Study of Pressure Pulses Generated by Travelling Bubble Cavitation, *J. Fluid Mech.*, **255**, 541-564

18. LANDAU L.D., LIFSHIC E.M., 1958, *Mechanics of Continuum Systems* (in Polish), PWN Warsaw

19. NAKORYAKOV V.E., POKUSAEV B.G., SHREIBER I.R., PRIBATURIN N.A., 1988, The Wave Dynamics of a Vapour-Liquid Medium, *Int. J. Multiphase Flow*, **14**, 655-677

20. NAKORYAKOV V.E., POKUSAEV B.G., SHREIBER I.R., 1993, *Wave Propagation in Gas-Liquid Media*, CRC Press, Florida

21. NIGMATULIN R.I., 1991, *Dynamics of Multiphase Flow*, Hemisphere

22. NOORDZIJ L., 1971, Shock Waves in Bubble-liquid Mixtures, Phys. Comm. Twente Univ. Techn., 3, 369-383, also in *Proc. IUTAM Symp. on Non-steady Flow of Water at High Speeds*, 1973 (edit. by L.I. Sedov, G. Yu-Stepanov), Nauka, Moscow, p.369

23. REOCREUX M., 1974, Contribution a l'etude des debits Critiques en ecoulement diphasique eau-vapeur, Ph.D. Thesis, Université Scientifique et Médicale de Grenoble, France

24. TRUESDELL C., NOLL W., 1965, *Handbuch der Physik* III/1, Edit. S. Flugge, Springer, Berlin

25. WHITHAM G.B., 1974, *Linear and Nonlinear Waves*, J. Wiley and Sons, New York

Nierównowaga termodynamiczna i mechaniczna w przepływie mieszaniny wody i pary z gwałtownym odparowaniem i falą uderzeniową

Streszczenie

Zawarto także wyniki badań eksperymentalnych stacjonarnej fali uderzeniowej w przeplywie wody i pary, które obejmowały pomiary parametrów przepływu wewnątrz obszaru zajmowanego przez falę. Dane doświadczalne wykorzystano do sprawdzenia założeń modelu matematycznego.

Manuscript received September 3, 1996; accepted for print February 6, 1997